Electronic spectra of positively charged carbon clusters - C_{2n}^+ (n=6-14)

Jack T. Buntine,[1] Mariah I. Cotter,[1] Ugo Jacovella,[1, a)] Chang Liu,[1] Patrick Watkins,[1] Eduardo Carrascosa,[1, b)] James N. Bull,[1, c)] Luke Weston,[1] Giel Muller,[1] Michael S. Scholz,[1, d)] and Evan J. Bieske[1, e)]

School of Chemistry, The University of Melbourne, Victoria,

Australia 3010

(Dated: 24 October 2021)

Electronic spectra are measured for mass-selected C_{2n}^+ (n=6-14) clusters over the visible and near infrared spectral range through resonance enhanced photodissociation of clusters tagged with N_2 molecules in a cryogenic ion trap. The carbon cluster cations are generated through laser ablation of a graphite disk, and can be selected according to their collision cross section with He buffer gas and their mass prior to being trapped and spectroscopically probed. The data suggest that the C_{2n}^+ (n=6-14) clusters have monocyclic structures with bicyclic structures becoming more prevalent for C_{22}^+ and larger clusters. The C_{2n}^+ electronic spectra are dominated by an origin transition that shifts linearly to longer wavelength with the number of carbon atoms, and associated progressions involving excitation of ring deformation vibrational modes. Bands for C_{12}^+, C_{16}^+, C_{20}^+, C_{24}^+ and C_{28}^+ are relatively broad, possibly due to rapid non-radiative decay from the excited state, whereas bands for C_{14}^+, C_{18}^+, C_{22}^+ and C_{26}^+ are narrower, consistent with slower non-radiative deactivation.

―――――――

[a)] Université Paris-Saclay, CNRS, France

[b)] Laboratoire de Chimie Physique Moléculaire, École Polytechnique Fédérale de Lausanne, EPFL SB ISIC LCPM, Station 6, CH-1015 Lausanne, Switzerland

[c)] School of Chemistry, Norwich Research Park, University of East Anglia, Norwich NR4 7TJ, United Kingdom

[d)] Department of Chemistry, University College London, London WC1H 0AJ, United Kingdom

[e)] Electronic mail: evanjb@unimelb.edu.au

I.   INTRODUCTION

Positively charged carbon clusters were first identified in mass spectrometric studies around 80 years ago,[1] and since then have been subject to extensive experimental and theoretical investigations concerned with their structures, reactivity and spectroscopic properties.[2,3] A significant outcome of these studies is a recognition of the structural diversity of carbon cluster cations.[4] Gas-phase ion mobility measurements have demonstrated that C_n^+ clusters formed through laser ablation of graphite exist as linear isomers for n=3-10, monocycles for $n \geq 7$, bicycles for $n \geq 21$ and fullerenes for $n \geq 30$.[4] The coexistence of linear and ring structures for smaller C_n^+ clusters ($n \leq 20$) was originally deduced on the basis of gas-phase reactivity studies from which it was concluded that linear clusters react rapidly with H_2,[5] D_2,[6,7] O_2,[6] CO, HCN, H_2O,[8] and hydrocarbons,[9] whereas the cyclic clusters react slowly, if at all, with these neutral species. Linear and cyclic isomers also decompose to different sized photofragments when exposed to 266 and 355 nm light.[10,11] The preference of mid-sized C_n^+ (n=10-18) clusters for cyclic rather than linear structures is consistent with electronic structure calculations.[12]

Spectroscopic studies of carbon cluster cations have mainly been restricted to species with fewer than ten carbon atoms, including C_6^+-C_9^+,[13,14] and the larger C_{60}^+ and C_{70}^+ fullerenes.[15–17] Significantly, the electronic spectrum of C_{60}^+ exhibits features that match four diffuse interstellar bands (DIBs).[15–18] Although mid-sized carbon cluster cations with 10-30 carbon atoms have been characterized through their abundance, drift mobility, photodissociation behaviour and reactivity, there have been few measurements of their infrared and electronic transitions, which are crucial for identifying the presence of these species in remote environments, including interstellar space. To address this paucity of spectroscopic data, we have recorded electronic spectra of C_{2n}^+ (n=6-14) clusters, embracing a size range where the positively charged carbon clusters exist mainly as monocycles with the alternative bicyclic structure becoming progressively more important for clusters larger than C_{22}^+.[4] The presence of co-existing monocyclic, bicyclic and possibly linear structures for the C_{2n}^+ (n=6-14) clusters presents challenges for measuring and interpreting electronic and infrared spectra, and ideally requires mass- and isomer-selective approaches to yield unambiguous spectra. To address these challenges, we have adopted an approach whereby, following their formation, the C_n^+ ions pass through a drift tube ion mobility spectrometer and then a quadrupole mass

filter, affording the capacity to separate and select the clusters on the basis of their collision cross sections with He buffer gas and their m/z. The gas-phase spectra are obtained by resonance enhanced photodissociation (REPD) of the target C_n^+ clusters tagged with N_2 molecules in a cryogenically cooled quadrupole ion trap.

To our knowledge, the only previous spectroscopic study of mid-sized carbon cluster cations was for C_{11}^+, C_{12}^+, C_{15}^+, C_{16}^+, C_{18}^+ and C_{21}^+ clusters that were generated by bombarding C_{60} with electrons, mass-selected and deposited in a Ne matrix where their electronic and infrared absorption spectra were measured.[19,20] The Ne matrix spectra also contained contributions from neutral, anion and fragment carbon clusters, potentially complicating their interpretation. Bands in the visible spectral region were assigned to linear carbon clusters as accompanying time dependent density functional theory (TD-DFT) calculations predicted that linear species absorb strongly in the visible spectral region, whereas cyclic isomers were calculated to possess strong absorptions below 250 nm.[20]

Experimental spectra of mid-sized carbon cluster cations with a controlled isomeric constitution, as obtained in the current study, should eventually help in elucidating the isomeric form of carbon clusters formed in different environments. For example, C_{12}^+ and C_{18}^+ clusters produced through dissociative ionization of overcrowded perchlorohydrocarbons exhibit the same reactivity and dissociation behaviour as clusters generated from the laser ablation of graphite, evidence that they share a common cyclic structure.[21] Also, it has been found that larger PAH cations such as hexa-peri-hexabenzocoronene ($C_{42}H_{18}^+$) exposed to intense pulses of visible light (λ=532 nm) lose peripheral H atoms to form cage structures and also smaller C_n^+ clusters with n=16-20.[22] Furthermore, exposing the coronene radical cation ($C_{24}H_{14}^+$) to UV radiation leads to complete dehydrogenation to form the C_{24}^+ cluster.[23] Comparison of the electronic spectra of carbon clusters formed through decomposition of PAHs with electronic spectra reported in the current study may help decide whether they retain the skeletal structure of the parent molecule, or isomerize to some other structure. These considerations are relevant in the context of the proposed widespread existence of PAHs in interstellar space where exposure to UV light may cause loss of H atoms and formation of bare carbon clusters.[23]

The current spectroscopic study of the C_{2n}^+ (n=6-14) clusters complements extensive spectroscopic investigations of related neutral and charged carbon clusters, which have been motivated by their role in a range of environments, including in comets, carbon stars and

interstellar molecular clouds, and in flames and furnaces.[2,3] For example, electronic spectra have also been measured for smaller C_6^+-C_9^+ clusters deposited in a Ne matrix, with observed transitions assigned to both linear and cyclic isomers,[13,14] and for C_6^+-He_n clusters in the gas phase.[24] Electronic spectra have been obtained for C_{60}^+ and C_{70}^+ fullerenes in Ne matrices,[25,26] and through REPD of C_{60}^+-He_n and C_{70}^+-He_n complexes in the gas-phase.[15–17] Gas-phase electronic spectra of C_{70}^{2+}-He_n complexes have been obtained by similar means.[27] Electronic spectra have been obtained for linear C_{2n} (n=3-7) and C_{2n+1} (n=2-10) clusters in a Ne matrix,[28–30] and for cyclic C_{14}, C_{18} and C_{22} molecules in the gas phase using resonance enhanced multiphoton photoionization.[31,32] Infrared spectra have been obtained for linear C_n clusters up to n=13 in the gas phase[3,33] and in a Ne matrix.[34] Ionization potentials for neutral C_n (n=2-15) clusters have been measured using tunable VUV radiation.[35] Negatively charged carbon clusters have been investigated using photoelectron spectroscopy,[36,37] matrix isolation spectroscopy,[29,38] and resonance enhanced photodetachment spectroscopy.[39]

Although carbon clusters have mainly been generated and characterized in the gas phase or in Ne matrixes, drawn by their predicted unique electronic and optical properties, synthetic chemists have sought to generate cyclocarbons in condensed phases.[40,41] One recent novel synthesis involved production of C_{18} on a cooled NaCl surface by elimination of CO molecules from the $C_{24}O_6$ cyclocarbon oxide molecule.[42] High resolution atomic force microscopy showed that C_{18} formed in this way has a cyclic polyynic structure, as predicted by electronic structure calculations.[43] Ultimately, gas-phase electronic spectra of cyclocarbon cations reported in this paper should provide useful data for benchmarking theoretical approaches, which, in turn, should help guide synthetic condensed-phase studies.

II. EXPERIMENTAL METHODS

Spectra of the C_n^+ clusters were obtained by REPD of cryogenically cooled C_n^+-$(N_2)_m$ complexes in a three-dimensional quadrupole ion trap (3D QIT). The C_n^+ clusters were generated by laser ablation of a rotating carbon disk using the focused, frequency-doubled output of a pulsed Nd:YAG laser (λ=532 nm, 12 mJ/pulse, 20 Hz). The ablation source is situated at the beginning of a drift tube ion mobility spectrometer with which, if required, the clusters can be separated according to their drift time through He buffer gas (P≈2 Torr) using a pulsed Bradbury-Nielsen ion gate located at the end of the drift region. Following

passage through the drift region, the charged clusters were collected by an RF ion funnel and passed through a 1 mm orifice into an RF hexapole ion guide (pressure typically 5×10^{-5} Torr), which was used to accumulate ions from 10 ablation laser pulses over 0.5 s. After their exit from the hexapole, the ions travelled through a quadrupole mass filter where they were mass-selected. The ions then passed through an octupole ion guide and into the QIT cooled to $T\approx20$ K into which pulses of a He/N_2 100:1 gas mixture were injected at 2 Hz. The C_n^+ clusters were tagged with N_2 molecules in the QIT before being ejected (after 480 ms) into a linear time-of-flight (ToF) mass spectrometer (length 0.9 m). Alternate packets of ions in the QIT were exposed to pulses of unfocused, wavelength-tunable light from an optical parametric oscillator (OPO, EKSPLA NT 342B, ≤ 1 mJ/cm^2/pulse, 6 ns pulse width, bandwidth≈ 4 cm^{-1}). The ions were typically exposed to a single pulse of light from the tunable OPO around 400 ms after their introduction into the trap at the end of the trapping cycle. The effect of the light was manifested in the difference between the light-on and light-off ToF mass spectra; when the OPO was tuned to a resonance, the C_n^+-$(N_2)_m$ signal diminished and the C_n^+ photofragment signal grew. As an example, FIG. 1 displays the difference ToF mass spectrum for C_{20}^+-$(N_2)_m$ with the OPO tuned to 897 nm (the origin band for C_{20}^+-N_2). Normally, the light intensity was adjusted so that $\leq 10\%$ of the N_2 tagged ions were dissociated. Where possible we attempted to obtain spectra with a range of laser powers to test whether power broadening was an issue.

Electronic spectra were obtained by plotting either the integrated C_n^+-$(N_2)_m$ photodepletion signal or the C_n^+ photofragment signal as a function of wavelength with intensities normalised by OPO power. Wavelength calibration was accomplished with a wavemeter (High Finesse, LSA). It is relevant to note that exposure to light over the visible and near-infrared range caused no appreciable photofragmentation of the core C_n^+ clusters.

III. RESULTS AND DISCUSSION

A. Ion mobility data

The isomeric composition of carbon clusters produced by the laser ablation source was assessed using the drift tube ion mobility spectrometer in which the ions were separated according to their collision cross section with the He buffer gas; compact ions travel more
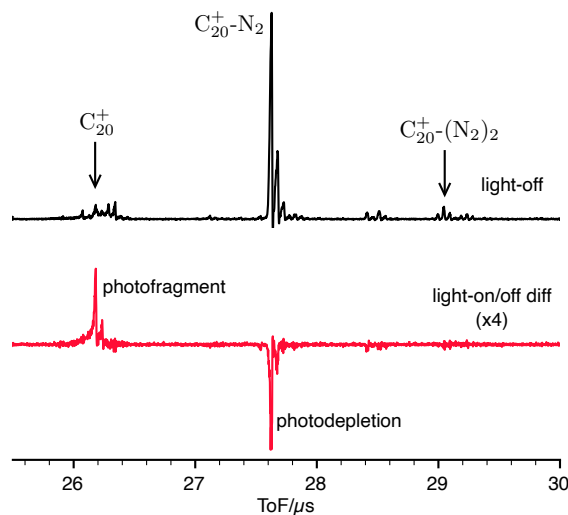
FIG. 1. Light-off and light-on/off difference ToF mass spectra for C_{20}^+-$(N_2)_m$ (m=0-2) clusters with the OPO tuned to 897 nm, the strongest absorption of C_{20}^+-N_2 in the visible/NIR.

quickly through the buffer gas and arrive at the detector earlier than extended ions. FIG. 2 shows a plot of ion current versus arrival time and m/z for C_n^+ clusters with n=10-60. The data demonstrate that the n=10-28 clusters are predominantly monocycles, with larger n=22-40 clusters existing as both monocycles and more compact bicycles, and with fullerenes becoming increasingly apparent for $n{\geq}32$. Families of multiply charged fullerenes (C_n^{2+}, C_n^{3+}, C_n^{4+}) are also evident at shorter arrival times. Relative abundances of the different clusters depend on ion source conditions, particularly the power of the ablation laser. Our ion mobility measurements are consistent with C_n^+ mobility data from von Helden *et al.*[4] For example, drift times for the monocyclic, bicyclic and fullerene isomers of C_{36}^+ have ratios of 1.93:1.76:1, close to drift time ratios calculated using the measured mobilities reported in ref. 4 (1.97:1.80:1).

For the spectroscopic investigations of the C_{12}^+ to C_{28}^+ clusters described below, the apparatus was normally run without mobility selection of the target complex because the monocyclic isomer is present in far greater abundance than the bicyclic isomer and the multiply charged fullerenes that share the same m/z. In support of this approach we conducted tests for C_{28}^+, and found that gating the slower C_{28}^+ ions, corresponding to the monocyclic isomer, gave rise to sharp peaks over the 1000-1400 nm wavelength range, whereas the faster C_{28}^+ ions associated with the bicyclic isomer did not absorb appreciably in this region.
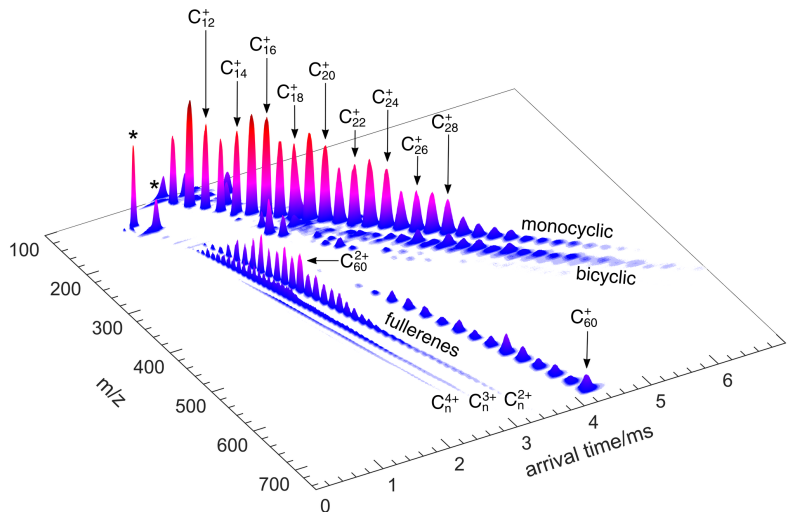
FIG. 2. Ion intensity versus drift time and m/z for C_n^+ clusters with conditions optimised for generation and detection of smaller clusters. Asterisked peaks with maxima at m/z 138 and 154 are tentatively assigned to impurity Ba^+, BaO^+ and $BaOH^+$ ions.

B.   Electronic spectra

Electronic spectra of C_{2n}^+ (n=6-14) carbon clusters tagged with N_2 molecules measured over the visible to NIR range are shown in FIG. 3. Presumably, the observed transitions are from the doublet ground state to the lowest lying doublet excited state of the clusters. Wavenumbers for the peaks are listed in Table I. Each of the C_{2n}^+ (n=6-14) spectra is dominated by an origin transition flanked by weaker peaks 300-600 cm^{-1} to higher energy that presumably correspond to vibronic progressions in ring deformation modes. The most striking feature of the C_n^+ spectra series is that the origin transition shifts linearly to longer wavelength with n (see FIG. 4). This, along with the ion mobility data shown in FIG. 2 constitutes strong evidence that the C_n^+ clusters responsible for the absorptions have a common structural motif. A similar linear dependence of absorption wavelength on cluster size has been observed for several different homologous linear carbon and species, including C_{2n}, C_{2n}^-, $C_{2n}H^-$,[30] C_{2n+1},[28] and $HC_{2n}H^+$.[44] Perhaps significantly, the wavelength for the $\tilde{E} \leftarrow \tilde{X}$ origin transition of cyclic C_8^+, previously measured at 336.5 nm in a Ne matrix, fits with the trend for the n=12-28 series.[14] We have unsuccessfully sought the transition for C_{10}^+, which, by extrapolation, is predicted to occur in a wavelength region where the output

7
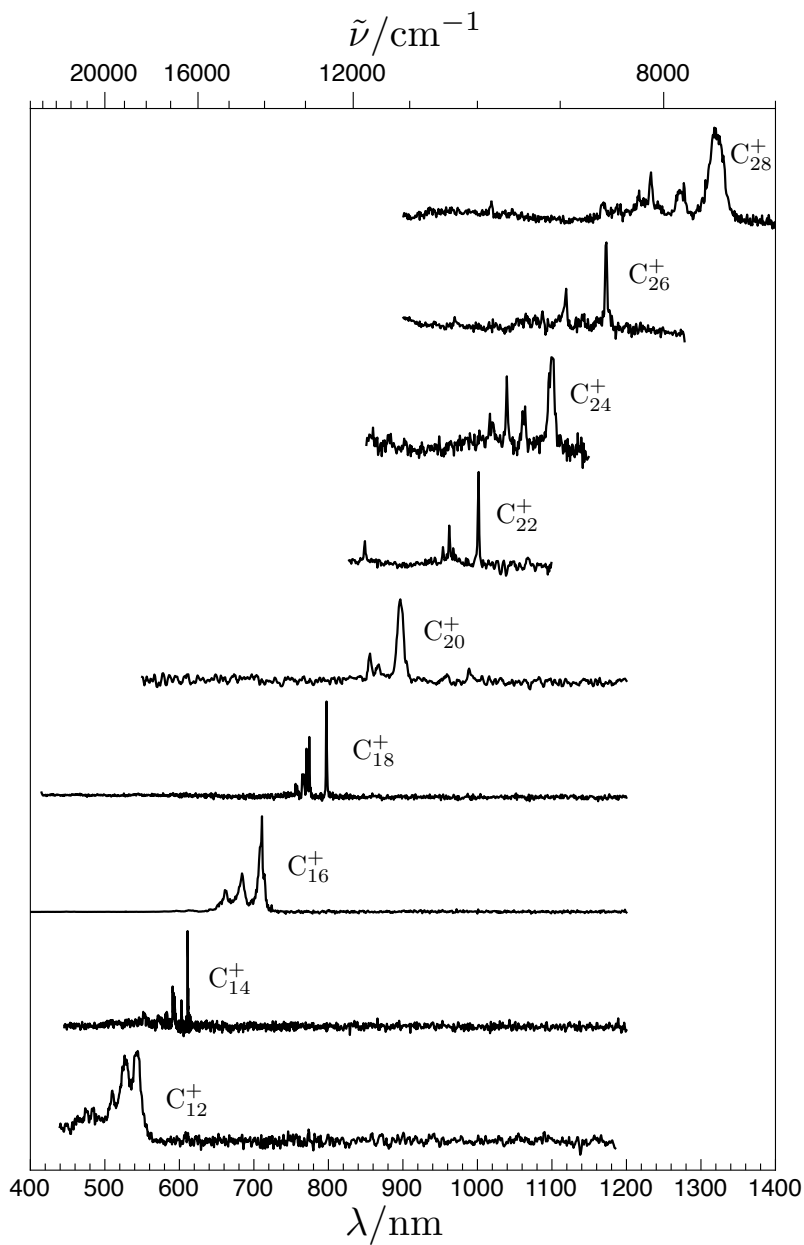
FIG. 3. Electronic spectra for C_n^+-$(N_2)_n$ clusters obtained by monitoring C_n^+ photofragments following laser excitation. The spectra, which are normalized with respect to OPO power, may be slightly saturated such that the intensities of weaker peaks are exaggerated with respect to the origin transition.

of the OPO is weak ($\approx 410\,\mathrm{nm}$).
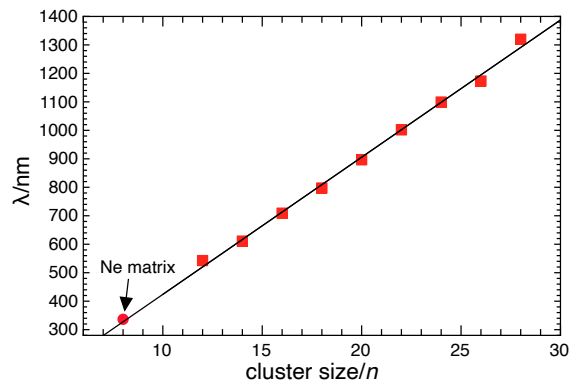
FIG. 4. Plot of the origin band wavelengths versus n for even C_n^+ clusters. The $n=8$ point at 336.5 nm corresponds to the $\tilde{E} - \tilde{X}$ origin transition of cyclic C_8^+ in a Ne matrix (from ref. 14).

TABLE I: Wavenumbers (cm^{-1}, vacuum) for transitions of C_n^+ clusters tagged with N_2 molecules. Positions are given for spectra obtained by monitoring formation of C_n^+ photofragments [resulting from photofragmentation of both C_n^+-N_2 and C_n^+-$(N_2)_2$], and from photodepletion spectra of C_n^+-N_2 and C_n^+-$(N_2)_2$. Uncertainties in positions depend on cluster size and are estimated as $\pm 40\,cm^{-1}$(n=12), $\pm 5\,cm^{-1}$ (n=14, 18, 22, 26), $\pm 20\,cm^{-1}$ (n=16, 20, 24, 28).

| | | mass channel monitored | | | | | |
| | | C_n^+ photofrag. | | C_n^+-N_2 depletion | | C_n^+-$(N_2)_2$ depletion | |
n	assignment	$\tilde{\nu}$	$\Delta\tilde{\nu}$	$\tilde{\nu}$	$\Delta\tilde{\nu}$	$\tilde{\nu}$	$\Delta\tilde{\nu}$
12	0_0^0	18426	0	18444	0	18481	0
		18934	508	18934	490	18988	507
		19621	1195	19659	1215	19699	1218
		-	-	-	-	20848	2367
14	0_0^0	16338	0	16338	0	16362	0
		16362	24	-	-	-	
		16585	247	16565	227	16590	228
		16830	492	-	-	16836	474
		16873	535	16849	511	16873	511
		16912	574			16921	559
16	0_0^0	14099	0	14090	0	14082	0
		14615	516	14615	525	14615	533
		15101	1002	15112	1022	15112	1030
18	0_0^0	12536	0	-	-	12536	0
		12910	374	-	-	12918	382
		12973	437	-	-	12973	437
		13053	517	-	-	13053	517
		13189	653	-	-	13189	653
		13225	689				
20	0_0^0	11151	0	11125	0	-	-
		11536	385	11510	385	-	-
		11694	543	11694	569	-	-
22	0_0^0	9981	0	9981	0	-	-
		10333	352	10333	352	-	-
		10390	409	10390	409	-	-

Continued on next page

TABLE I – *Continued from previous page*

n	assignment	C_n^+ photofrag. $\tilde{\nu}$	C_n^+ photofrag. $\Delta\tilde{\nu}$	C_n^+-N_2 depletion $\tilde{\nu}$	C_n^+-N_2 depletion $\Delta\tilde{\nu}$	C_n^+-$(N_2)_2$ depletion $\tilde{\nu}$	C_n^+-$(N_2)_2$ depletion $\Delta\tilde{\nu}$
		10482	501	10482	501	-	-
		11775	1794	11775	1794	-	-
24	0_0^0	9094	0	9094	0	-	-
		9416	322	9416	322	-	-
		9618	524	9618	524	-	-
		9804	710	9813	719	-	-
26	0_0^0	8522	0	8522	0	8522	0
		8933	411	8942	420	8951	429
28	0_0^0	7576	0	7570	0	-	-
		7855	279	7837	267	-	-
		8117	541	8110	540	-	-

There are several reasons to believe that the absorptions shown in FIG. 3 are due to monocyclic C_n^+ clusters. First, as noted above, the ion mobility data for the C_n^+ clusters with $n \geq 10$ are similar to previously reported measurements,[4] and are consistent with monocyclic structures for n=10-20 and the coexistence of monocyclic and bicyclic structures for n=22-28. Second, for clusters with $n \geq 10$ the monocyclic clusters are calculated to lie considerably lower in energy than the linear clusters.[12] For example, cyclic C_{16}^+ is calculated to be 3.24 eV more stable than linear C_{16}^+ at the ωB97X-D/cc-pVTZ level of density functional theory (DFT). Third, linear clusters, if they do form through isomerization of cyclic clusters following their passage through the ion mobility spectrometer drift region - either when they were stored in the hexapole, passing through the octopole ion guide, or contained in the cryogenic QIT - would be expected to react rapidly with trace H_2O or H_2 to form linear C_nH^+ or HC_nH^+ molecules.[5–8] We tested this by recording spectra of the C_n^+ clusters with both H_2/N_2 (100:1) and He/N_2 (100:1) buffer gas mixtures in the QIT and found no substantial differences in ToF mass spectra or in the electronic spectra. Last, preliminary experiments with mobility selection of the C_n^+ clusters clearly show that the spectral features apparent in FIG. 3 are associated with the slower, less compact monocyclic clusters rather than with

11

the faster, more compact bicyclic clusters. Furthermore, when the bicyclic clusters were selected there was no trace of the sharp spectral features indicating that collision-induced bicylic→monocyclic isomerization does not occur following mobility selection of the clusters in the drift region.

Some of the transitions measured for C_n^+ clusters in the gas phase correspond to bands previously reported for mass-selected C_n^+ clusters in a Ne matrix, where the ions were generated by subjecting C_{60} vapour to electron impact.[19,20] For example, the strongest bands in the gas-phase C_{16}^+ spectrum at 710.87 and 684.05 nm (FIG. 3) correspond in positions and relative intensities to prominent, unassigned peaks near 710 and 685 nm in the Ne matrix spectrum obtained when C_{16}^+ was mass-selected and deposited (FIG. S12 in the Supporting Information for ref. 20). Furthermore, the strongest bands in the gas-phase spectrum for C_{20}^+ shown in FIG. 3 at 896.5 nm and 854.9 nm correspond in position and relative intensities to peaks at 899 and 857 nm reported in ref. 19 for carbon cluster cations with m/z 240 deposited in a Ne matrix, which were attributed to C_{60}^{3+}. For the following reasons, the species responsible for the absorptions is almost certainly C_{20}^+ rather than C_{60}^{3+}. First, the ion mobility data show that for typical operating conditions the laser ablation ion source produces relatively small quantities of C_{60}^{3+} compared to C_{20}^+ (see FIG. 2). Second, the ToF mass peak for the m/z 240 species tagged with N_2, which was irradiated to obtain the gas-phase spectrum, appears at m/z 268 (as expected for C_{20}^+-N_2) rather than at m/z 249.3 (where it would be for C_{60}^{3+}-N_2). Finally, the wavelength of the origin band at 896.5 nm fits the pattern established for the other C_n^+ clusters (see FIG. 4), which are certainly not multiply charged fullerenes.

There are few theoretical predictions for the transition energies of monocyclic C_n^+ clusters that can be compared with the experimental data reported here. Although large-scale multi-reference configuration interaction (MRD-CI) calculations have been carried out for the smaller C_6^+ and C_8^+ clusters and predict electronic transitions with weak to medium intensity occur across the visible and NIR spectral range,[45] calculations of similar quality are unavailable for larger cyclic clusters. TD-DFT calculations reported in ref. 20 predict that cyclic C_n^+ (n=10-20) clusters have very strong transitions below 250 nm with oscillator strengths ranging from 1.4 to 7.7. Wavelengths for transitions occurring in the visible region, which were calculated to be relatively weak, were not reported.[20]
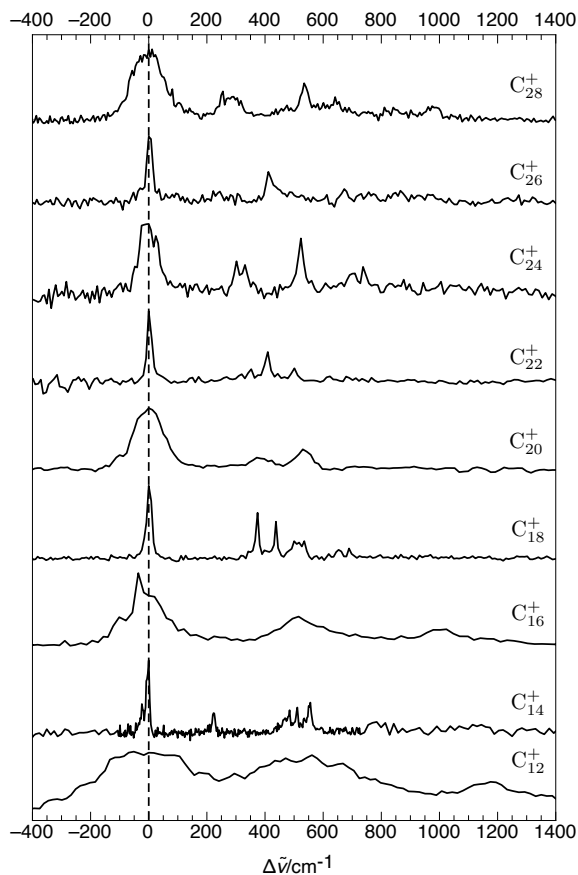
C. Vibronic structure

FIG. 5. Expanded view of the spectra for C_n^+ clusters. The dashed vertical line represents the positions of the aligned origin bands for the C_n^+ clusters.

In each of the C_n^+ spectra, the strongest band is flanked by weaker peaks lying 300-600 cm^{-1} to higher energy that are presumably associated with progressions involving the low frequency ring vibrational modes. These spectral features can be appreciated in FIG. 5 where the origin bands for the different C_n^+ clusters are aligned. Calculated vibrational frequencies for C_{12}^+, C_{14}^+ and C_{16}^+ in their ground electronic states are given in the Supplemental Material. Assigning these peaks to particular vibrational modes is difficult, given that the geometry and vibrational frequencies for the clusters in their excited electronic states are unknown, and because of the large number of low frequency vibrational modes. For example, C_{14}^+ has 15 in-plane vibrational modes lying below 1000 cm^{-1} (see Table S7 in the Supplementary Material). One can only say that if the rings have a cumulenic structure with equal C=C bond lengths and C=C=C bond angles in the ground and excited states (D_{nh} symmetry) then

13

the band systems should only exhibit progressions in the totally symmetric ring expansion mode. Presence of additional peaks indicates that the molecules have a lower symmetry in one or both of these electronic states.

D.   Effect of N_2 tag molecules

Because the spectra are obtained through resonance enhanced photodissociation of C_n^+-$(N_2)_m$ clusters, it is relevant to consider the effect of the attached N_2 molecule(s) on the structures and transition energies of the carbon clusters. DFT calculations conducted as part of this study at the ωB97X-D/aug-cc-pVDZ level of theory suggest that for cyclic clusters up to C_{18}^+, an attached N_2 molecule prefers to sit above or below the ring (see FIG. 6), but that for C_{19}^+ and larger clusters, a single N_2 molecule can be accommodated inside the ring. Typically, the N_2 molecules are bound by several hundred cm^{-1}. For example, the binding energy of N_2 to C_{14}^+ is calculated to be $790\,cm^{-1}$, with the second N_2 bound by a similar amount ($775\,cm^{-1}$). The dissociation energy of C_{20}^+-N_2, for which the N_2 molecule resides inside the ring, is calculated to be slightly higher ($984\,cm^{-1}$). The attached N_2 molecules are predicted to have a minor effect on the vibrational frequencies of the core C_n^+ clusters, with shifts of less than $20\,cm^{-1}$ (see Table S7 in the Supplemental Information for calculated frequencies of C_{14}^+, C_{14}^+-N_2 and C_{14}^+-$(N_2)_2$). Frequencies of the intermolecular modes involving relative motion of the ring and N_2 molecule have relatively low calculated harmonic frequencies (for example, 13, 49, 67, 78, $97\,cm^{-1}$ for C_{14}^+-N_2). The absence of progressions with peak spacings less than $100\,cm^{-1}$ in the electronic spectra indicates that the interaction between the C_n^+ and N_2 molecule is largely unaffected by electronic excitation.

In some instances we have managed to measure spectra of both C_n^+-N_2 and C_n^+-$(N_2)_2$ clusters. For example, FIG. 7 shows photodepletion action spectra for C_{14}^+-N_2 and C_{14}^+-$(N_2)_2$, which have origin peaks at 611.9 and 611.0 nm, respectively. Assuming that each of the two attached N_2 molecules causes the same spectral shift, as expected for the structures shown in FIG. 6, the origin transition of the bare C_{14}^+ cluster would lie at 612.8 nm.
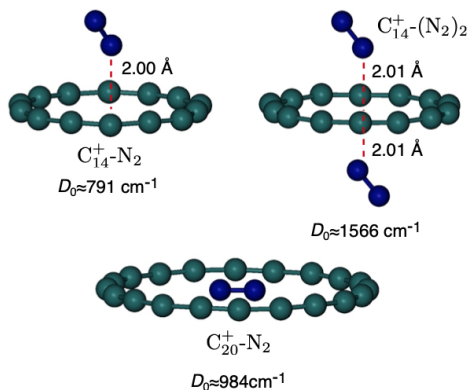
FIG. 6. Minimum energy structures for C_{14}^+-N_2, C_{14}^+-$(N_2)_2$ and C_{20}^+-N_2 showing the N_2 tag molecule sitting above and below the plane of the ring for C_{14}^+ and located in the middle of the ring for C_{20}^+. Distances are given from the closest N atom to the plane of the ring.
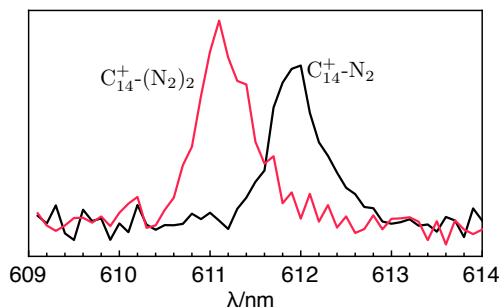

FIG. 7. Origin transitions for photodepletion spectra of C_{14}^+-N_2 and C_{14}^+-$(N_2)_2$.

E.   Transition bandwidths

A distinctive feature of the spectral series shown in FIGS. 3 and 5 is that the transitions for the C_{4k}^+ and C_{4k+2}^+ clusters have different widths. Electronic spectra of the C_{4k+2}^+ clusters (C_{14}^+, C_{18}^+, C_{22}^+, C_{26}^+) exhibit relatively sharp peaks (FWHM 10-20 cm^{-1}), whereas peaks for the C_{4k}^+ clusters (C_{12}^+, C_{16}^+, C_{20}^+, C_{24}^+, C_{28}^+) are noticeably broader (FWHM>100 cm^{-1}). The peak profiles will be influenced to some extent by the presence of the attached N_2 molecule(s) due to hot band transitions involving low frequency intermolecular modes. However, the broadening from this source should be similar for both series of clusters. A possible explanation for the broader peaks for the C_{4k}^+ clusters involves lifetime broadening associated with rapid nonradiative deactivation through intersystem crossing (ISC). The

15

lowest quartet state for the C_{4k}^+ clusters is calculated to lie just above the doublet ground state (by 0.4 eV for both C_{12}^+ and C_{16}^+ according to DFT calculations[12]), such that there should be a high density of quartet vibronic states iso-energetic with the excited doublet state, facilitating rapid intersystem crossing. In contrast, the lowest quartet state for the C_{4k+2}^+ clusters is predicted to lie much higher above the ground state (by 3.5 eV for C_{10}^+, 2.7 eV for C_{14}^+, 1.5 eV for C_{18}^+) so that there should be lower densities of quartet vibrational states iso-energetic with the excited doublet states and consequently lower ISC crossing rates.

F.   Comparison with DIBs

Given that the bands of the C_{12}^+-C_{28}^+ clusters span the visible to near infrared region of the spectrum, it is appropriate to consider whether any of the cyclic C_n^+ clusters are carriers of diffuse interstellar bands. Carbon cluster cations can conceivably form in the interstellar medium through a process whereby positively charged polyaromatic hydrocarbons progressively lose H atoms and rearrange following absorption of UV photons,[23] leading to bare dehydrogenated C_n^+ clusters, which, over the n=10-28 range, may have monocyclic structures. Electronic spectra of the neutral carbon rings C_{14}, C_{18} and C_{22} have previously been recorded, but no convincing match was found between the measured peaks and any DIBs.[31,32] Although the bands of the C_{4k}^+ series are probably too broad to be associated with DIBs, several of the C_{4k+2}^+ clusters exhibit sharper transitions that are close to DIBs. For example, six DIBs have been measured over the 610-613 nm range in the spectrum for HD 183143 (at 611.079, 611.329, 611.684, 611.874, 612.443, 612.820 nm),[46] nearby the strongest peak for C_{14}^+-N_2 at 611.9 nm. However, even if the origin transition of the C_{14}^+ band corresponds to one of these DIBs there are no reported DIBs with appropriate spacings, relative intensities and widths to explain the two shorter wavelength transitions (at 603.5 and 593.3 nm for C_{14}^+-N_2). A similar situation pertains for C_{18}^+. The most intense transition of C_{18}^+-$(N_2)_2$ occurs at 797.5 nm, nearby DIBs for HD 183143 at 796.809 nm and 797.192 nm.[46] However, there are no appropriate matches for the C_{18}^+-$(N_2)_2$ transitions near 773.9 and 770.6 nm. Ultimately, spectral shifts associated with the N_2 tag molecules make absolute comparisons with astronomical data impossible, and higher resolution spectra of the bare clusters are required to decide whether any of the C_n^+ clusters are carriers for DIBs.

IV.   CONCLUSIONS AND OUTLOOK

In summary, we have obtained electronic spectra of the C_{2n}^+ (n=6-14) clusters, which the available evidence suggests have monocyclic structures, and which, aside from the fullerenes, include the largest carbon clusters for which electronic spectra have been measured. The most remarkable feature of the series is the linear dependence of the origin transition wavelength on the number of carbon atoms in the cluster. Although the wavelengths for the absorptions of the C_n^+-$(N_2)_m$ clusters will be shifted slightly from those of the bare C_n^+ clusters, the spectra reported in this paper should provide a foundation for future measurements for C_n^+ clusters tagged by He or tag-free spectra to determine whether the absorptions correspond to DIBs.

The C_n^+ spectra reported in this paper also provide a new route for identifying the isomeric constitution of charged carbon clusters generated through decomposition of larger carbon-bearing molecules and clusters. Carbon clusters in the C_{12}^+ to C_{28}^+ range have been produced through dehydrogenation of PAHs,[23,47] from overcrowded perchloro hydrocarbons,[21] and electron impact of C_{60}^+.[20] In principle, electronic spectra of C_n^+ clusters generated in these different ways can be compared with spectra presented in this study to see whether the product clusters are monocycles or have some other structure.

There are several avenues to extend the spectroscopic investigations. First, it would be interesting to examine larger clusters for which there is a coexistence of monocyclic, bicyclic and fullerene structures (for example C_{36}^+). It remains to be seen whether bicyclic C_n^+ structures give rise to an orderly series of electronic absorptions as found for linear and ring structures. One complication for clusters with 30 or more carbon atoms is the existence of different isomers with similar collision cross sections but which have distinct structures and electronic spectra. For example, bicyclic C_{32}^+ may have an isomer with 16 atoms in each ring, and another isomer with 14 atoms in one ring and 18 atoms in the other. Such isomers should have distinct electronic spectra, but may be difficult to separate using ion mobility techniques.

Development of robust theoretical treatments that properly describe the ground and excited state properties of the C_n^+ clusters is desirable but represents an ongoing challenge. While density functional theory methods to obtain cluster geometries followed by time-dependent frameworks for electronic transition wavelengths and intensities might seem

computationally tractable, recent studies on a range of carbon clusters have highlighted erroneous results when using many density functionals in standard computational software packages, including not correctly describing the change in bond length alternation for either linear or cyclic isomers with cluster size.[43,48,49] Furthermore, accurate calculations are potentially complicated by Jahn-Teller effects[50] and for cations require open-shell methods which are notorious for wavefunction convergence difficulties. Hopefully these difficulties will be resolved so that theory can better guide the interpretation of experimental spectroscopic data.

SUPPLEMENTARY MATERIAL

The supplementary material contains details of the density functional theory calculations and includes calculated equilibrium structures and vibrational frequencies for C_{12}^+, C_{14}^+, C_{16}^+ and C_{20}^+.

ACKNOWLEDGMENTS

CONFLICT OF INTEREST

The authors have no conflicts to disclose.

DATA AVAILABILITY STATEMENT

The data that support the findings of this study are available from the corresponding author upon reasonable request.
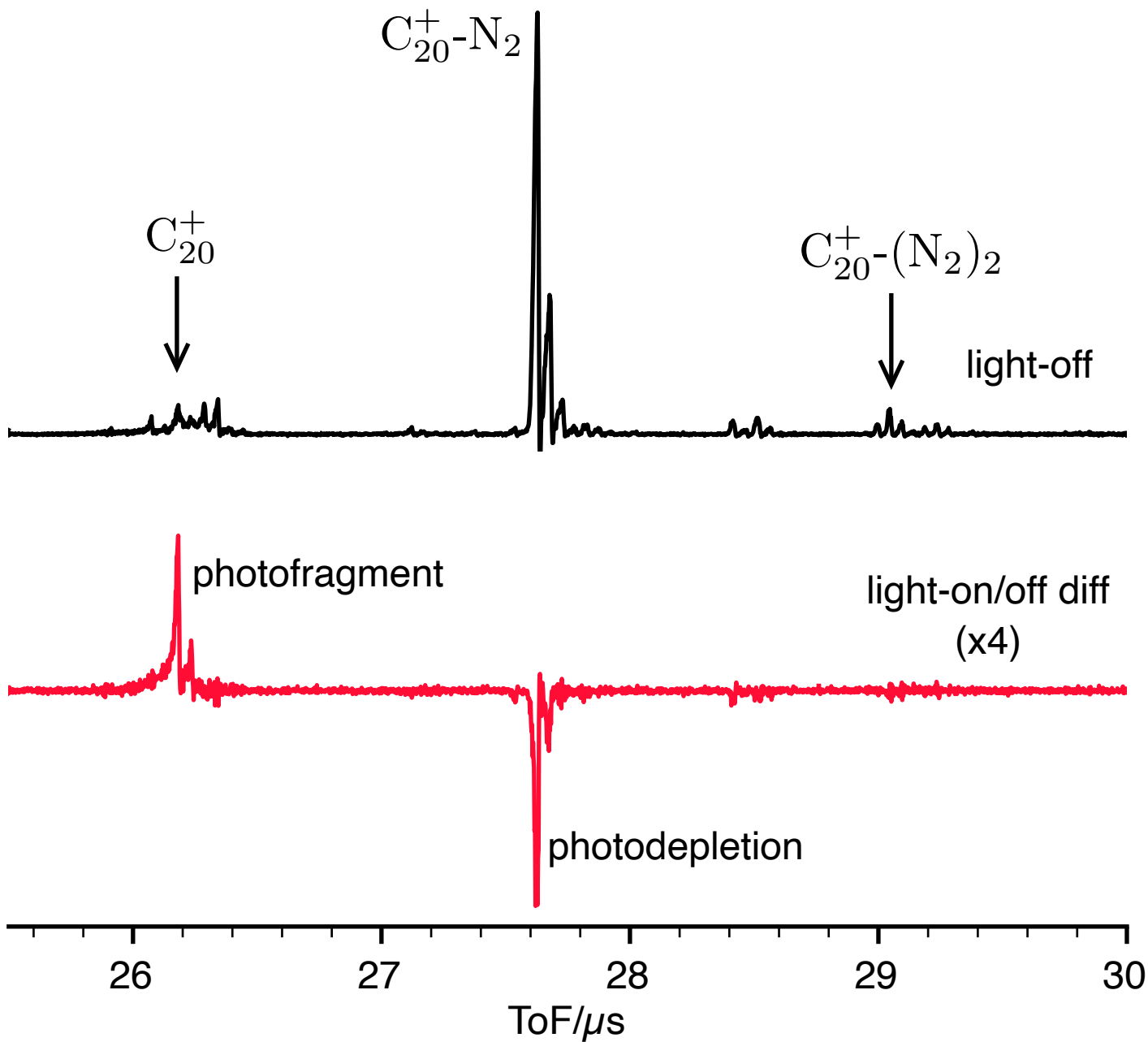
REFERENCES

[1] O. Hahn, F. Strassmann, J. Mattauch, and H. Ewald, "Hat in früheren Erdperioden ein radioaktives Cäsium existiert? Barium und Strontium aus Pollucit," Naturwissenschaften **30**, 541–542 (1942).

[2] W. Weltner and R. J. Van Zee, "Carbon molecules, ions, and clusters," Chem. Rev. **89**, 1713–1747 (1989).

[3] A. Van Orden and R. J. Saykally, "Small carbon clusters: Spectroscopy, structure, and energetics," Chem. Rev. **98**, 2313–2357 (1998).

[4] G. von Helden, M. T. Hsu, N. Gotts, and M. T. Bowers, "Carbon cluster cations with up to 84 atoms: Structures, formation mechanism, and reactivity," J. Phys. Chem. **97**, 8182–8192 (1993).

[5] D. K. Bohme and S. Wlodek, "Hydrogenation of carbon-cluster cations with molecular hydrogen: implications for the growth of carbon-cluster molecules," Int. J. Mass. Spectrom. Ion Proc. **102**, 133–149 (1990).

[6] S. W. McElvany, B. I. Dunlap, and A. O'Keefe, "Ion molecule reactions of carbon cluster ions with D_2 and O_2," J. Chem. Phys. **86**, 715–725 (1998).

[7] K. Koyasu, T. Ohtaki, J. Bing, K. Takahashi, and F. Misaizu, "Even-odd product variation of the $C_n^+ + D_2$ (n = 4-9) reaction: complexity of the linear carbon cation electronic states." Phys. Chem. Chem. Phys. **17**, 24810–24819 (2015).

[8] J. R. Heath, Q. Zhang, S. C. O'Brien, R. F. Curl, H. W. Kroto, and R. E. Smalley, "The formation of long carbon chain molecules during laser vaporization of graphite," J. Am. Chem. Soc. **109**, 359–363 (2002).

[9] S. W. McElvany, "Reactions of carbon cluster ions with small hydrocarbons," J. Chem. Phys. **89**, 2063–2075 (1998).

[10] K. Koyasu, T. Ohtaki, N. Hori, and F. Misaizu, "Isomer-resolved dissociation of small carbon cluster cations, C_7^+–C_{10}^+," Chem. Phys. Lett. **523**, 54–59 (2012).

[11] R. Moriyama, T. Ohtaki, J. Hosoya, K. Koyasu, and F. Misaizu, "Isomer-separated photodissociation of large sized silicon and carbon cluster ions: Drift tube experiment combined with a tandem reflectron mass spectrometer for Si_{24}^+ - Si_{27}^+ and C_{32}^+-C_{38}^+," Eur. Phys. J. D **67**, 1446–5 (2013).

[12]M. G. Giuffreda, M. S. Deleuze, and J. P. François, "Structural, rotational, vibrational, and electronic properties of ionized carbon clusters C_n^+ (n= 4-19)," J. Phys. Chem. A **103**, 5137–5151 (1999).

[13]J. Fulara, E. Riaplov, A. Batalov, I. Shnitko, and J. P. Maier, "Electronic and infrared absorption spectra of linear and cyclic C_6^+ in a neon matrix," J. Chem. Phys. **120**, 7520–7525 (2004).

[14]J. Fulara, I. Shnitko, A. Batalov, and J. P. Maier, "Electronic absorption spectra of linear and cyclic C_n^+ n=7-9 in a neon matrix." J. Chem. Phys. **123**, 044305 (2005).

[15]E. K. Campbell, M. Holz, D. Gerlich, and J. P. Maier, "Laboratory confirmation of C_{60}^+ as the carrier of two diffuse interstellar bands," Nature **523**, 322–323 (2015).

[16]E. K. Campbell, M. Holz, J. P. Maier, D. Gerlich, G. A. H. Walker, and D. Bohlender, "Gas phase absorption spectroscopy of C_{60}^+ and C_{70}^+ in a cryogenic ion trap: Comparison with astronomical measurement," Astrophys. J. **822**, 17 (2016).

[17]M. Kuhn, M. Renzler, J. Postler, S. Ralser, S. Spieler, M. Simpson, H. Linnartz, A. G. G. M. Tielens, J. Cami, A. Mauracher, Y. Wang, M. Alcamí, F. Martín, M. K. Beyer, R. Wester, A. Lindinger, and P. Scheier, "Atomically resolved phase transition of fullerene cations solvated in helium droplets," Nat. Commun. **7**, 13550 (2016).

[18]M. A. Cordiner, H. Linnartz, N. L. J. Cox, J. Cami, F. Najarro, C. R. Proffitt, R. Lallement, P. Ehrenfreund, B. H. Foing, T. R. Gull, P. J. Sarre, and S. B. Charnley, "Confirming interstellar C_{60}^+ using the Hubble space telescope," Astrophys. J. **875**, L28 (2019).

[19]B. Kern, D. Strelnikov, P. Weis, A. Böttcher, and M. M. Kappes, "IR, NIR, and UV absorption spectroscopy of C_{60}^{2+} and C_{60}^{3+} in neon matrixes," J. Phys. Chem. Lett. **5**, 457–460 (2014).

[20]D. V. Strelnikov, M. Link, J. Weippert, and M. M. Kappes, "Optical spectroscopy of small carbon clusters from electron-impact fragmentation and ionization of fullerene - C_{60}," J. Phys. Chem. A **123**, 5325–5333 (2019).

[21]C. Lifshitz, T. Peres, and I. Agranat, "Properties of carbon cluster ions, C_n^+, formed by dissociative ionization," Int. J. Mass. Spectrom. Ion Proc. **93**, 149–163 (1989).

[22]J. Zhen, D. Paardekooper, A. Candian, H. Linnartz, and A. Tielens, "Quadrupole ion trap/time-of-flight photo-fragmentation spectrometry of the hexa-peri-hexabenzocoronene (HBC) cation," Chem. Phys. Lett. **592**, 211–216 (2014).
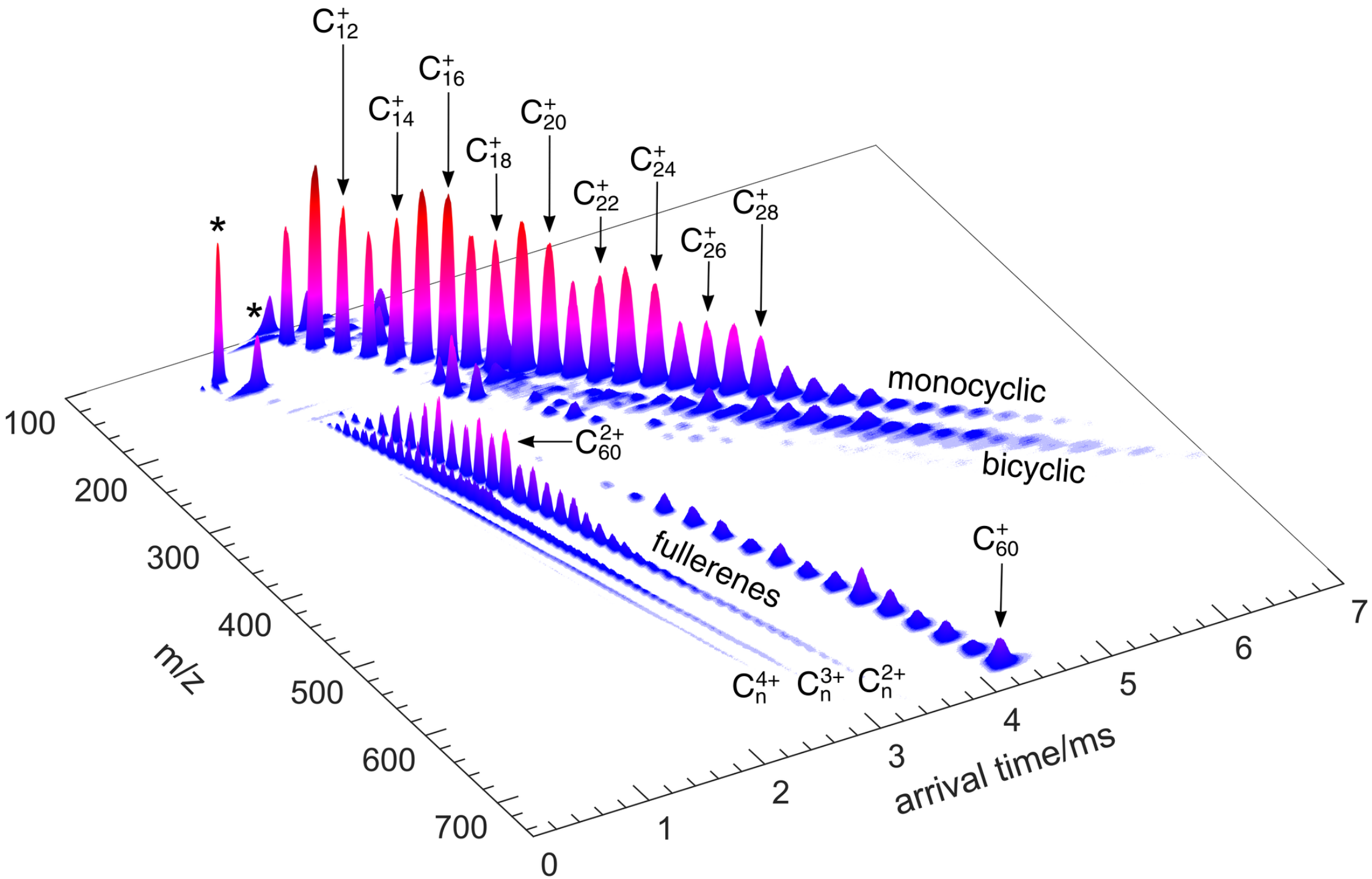
[23]S. P. Ekern, A. G. Marshall, J. Szczepanski, and M. Vala, "Photodissociation of gas-phase polycylic aromatic hydrocarbon cations," J. Phys. Chem. A **102**, 3498–3504 (1998).

[24]E. K. Campbell and P. W. Dunk, "LV-DIB-s4PT: A new tool for astrochemistry," Rev. Sci. Instr. **90**, 1–7 (2019).

[25]J. Fulara, M. Jacobi, and J. P. Maier, "Electronic and infrared spectra of C_{60}^+ and C_{60}^- in neon and argon matrices," Chem. Phys. Letts. **211**, 227–234 (1993).

[26]J. Fulara, M. Jakobi, and J. P. Maier, "Electronic spectra of the C_{70} molecule and C_{70}^+, C_{70}^- ions in neon matrices," Chem. Phys. Lett. **206**, 203–209 (1993).

[27]E. K. Campbell, M. Holz, and J. P. Maier, "Gas-phase absorption of C_{70}^{2+} below 10 K: Astronomical implications," Astrophys. J. **835**, 221 (2017).

[28]D. Forney, P. Freivogel, M. Grutter, and J. P. Maier, "Electronic absorption spectra of linear carbon chains in neon matrices. IV. $C_{2n+1} \, n = 2-7$," J. Chem. Phys. **104**, 4954–4960 (1996).

[29]M. Wyss, M. Grutter, and J. P. Maier, "Electronic spectra of long odd-number carbon chains C_{17} - C_{21} and C_{13}^- - C_{21}^-," Chem. Phys. Lett. **304**, 35–38 (1999).

[30]P. Freivogel, J. Fulara, M. Jakobi, D. Forney, and J. P. Maier, "Electronic absorption spectra of linear carbon chains in neon matrices. II. C_{2n}^-, C_{2n} and C_{2n}^-H," J. Chem. Phys. **103**, 54–59 (1995).

[31]A. E. Boguslavskiy, H. Ding, and J. P. Maier, "Gas-phase electronic spectra of C_{18} and C_{22} rings," J. Chem. Phys. **123**, 034305 (2005).

[32]A. E. Boguslavskiy and J. P. Maier, "Gas-phase electronic spectrum of the C_{14} ring," Phys. Chem. Chem. Phys. **9**, 127–130 (2007).

[33]P. Neubauer-Guenther, T. Giesen, U. Berndt, G. Fuchs, and G. Winnewisser, "The Cologne carbon cluster experiment: ro-vibrational spectroscopy on C_8 and other small carbon clusters," Spectrochim. Acta A Mol. Biomol. Spectrosc. **59**, 431–441 (2003).

[34]C. J. E. Straatsma, M. I. Fabrikant, G. E. Douberly, and H. J. Lewandowski, "Production of carbon clusters C_3 to C_{12} with a cryogenic buffer-gas beam source," J. Chem. Phys. **147**, 124201 (2017).

[35]L. Belau, S. E. Wheeler, B. W. Ticknor, M. Ahmed, S. R. Leone, W. D. Allen, H. F. Schaefer, and M. A. Duncan, "Ionization thresholds of small carbon clusters: Tunable VUV experiments and theory," J. Am. Chem. Soc. **129**, 10229–10243 (2007).
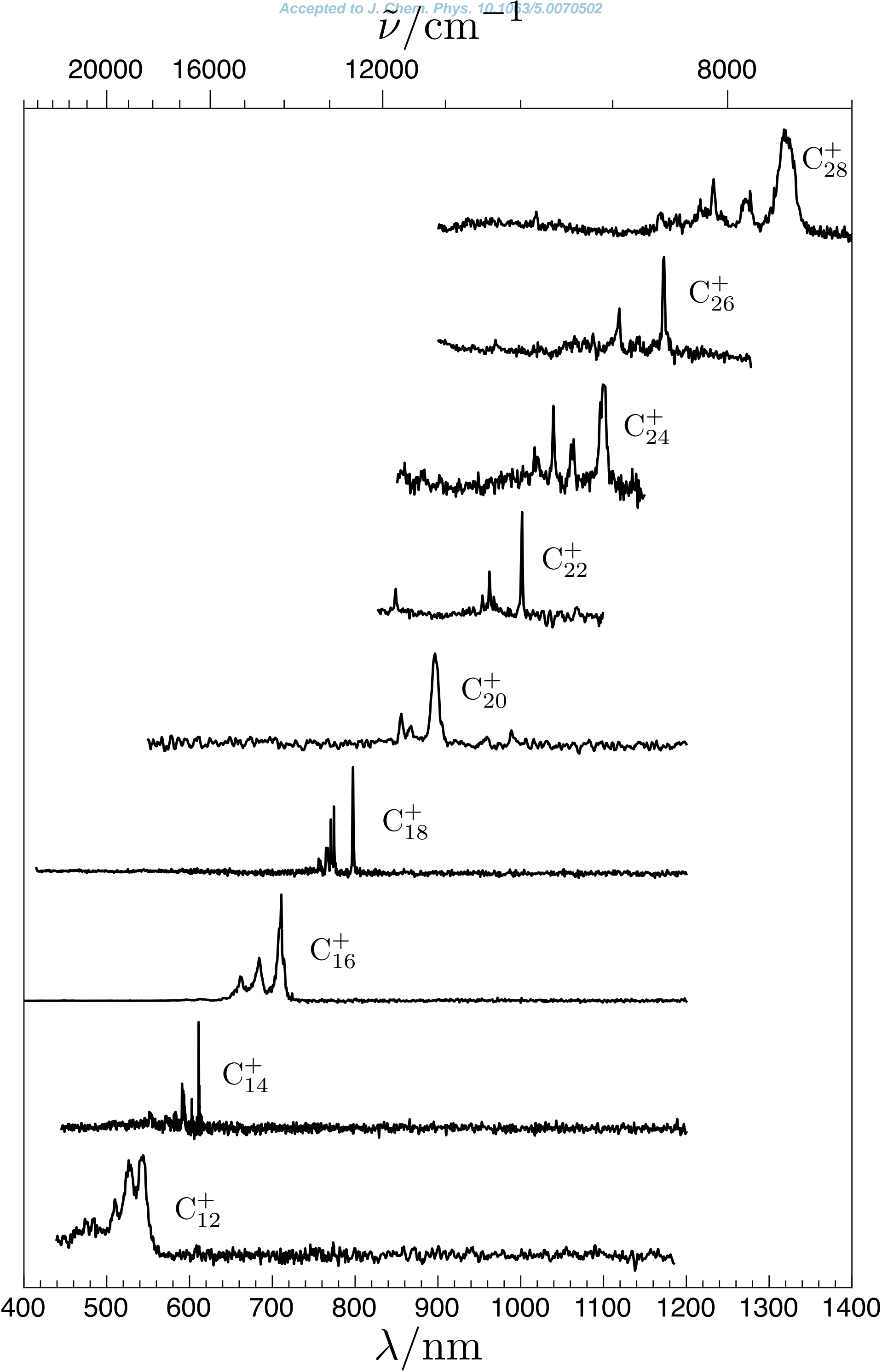
[36] D. W. Arnold, S. E. Bradforth, T. N. Kitsopoulos, and D. M. Neumark, "Vibrationally resolved spectra of C_2 - C_{11} by anion photoelectron spectroscopy," J. Chem. Phys. **95**, 8753–8764 (1991).

[37] M. C. Babin, J. A. DeVine, M. L. Weichman, and D. M. Neumark, "Slow photoelectron velocity-map imaging of cold C_7^- and C_9^-," J. Chem. Phys. **149**, 174306 (2018).

[38] P. Freivogel, M. Grutter, D. Forney, and J. P. Maier, "Electronic absorption spectra of carbon chain anions C_{2n}^- (n=4-7) in neon matrices," J. Chem. Phys. **107**, 4468–4472 (1997).

[39] M. Ohara, D. Kasuya, H. Shiromaru, and Y. Achiba, "Resonance-enhanced multiphoton electron detachment (REMPED) study of carbon anions up to C_{21}^-," J. Phys. Chem. A **104**, 8622–8626 (2000).

[40] F. Diederich, Y. Rubin, C. B. Knobler, R. L. Whetten, K. E. Schriver, K. N. Houk, and Y. Li, "All-carbon molecules: Evidence for the generation of cyclo[18]carbon from a stable organic precursor," Science **245**, 1088–1090 (1989).

[41] H. L. Anderson, C. W. Patrick, L. M. Scriven, and S. L. Woltering, "A short history of cyclocarbons," Bull. Chem. Soc. Jpn. **94**, 798–811 (2021).

[42] K. Kaiser, L. Scriven, F. Schulz, P. Gawel, L. Gross, and H. Anderson, "An sp-hybridized molecular carbon allotrope, cyclo[18]carbon," Science **365**, 1299–1301 (2019).

[43] G. V. Baryshnikov, R. R. Valiev, R. T. Nasibullin, D. Sundholm, T. Kurten, and H. Ågren, "Aromaticity of even-number cyclo[n]carbons (n= 6 - 100)," J. Phys. Chem. A **124**, 10849–10855 (2020).

[44] P. Freivogel, J. Fulara, D. Lessen, D. Forney, and J. P. Maier, "Absorption spectra of conjugated hydrocarbon cation chains in neon matrices," Chem. Phys. **189**, 335–341 (1994).

[45] J. Haubrich, M. Mühlhäuser, and S. D. Peyerimhoff, "A comparative MRD-CI study of the electronic spectrum of linear and cyclic C_8^+ clusters," J. Mol. Spec. **228**, 31–37 (2004).

[46] L. M. Hobbs, D. G. York, J. A. Thorburn, T. P. Snow, M. Bishof, S. D. Friedman, B. J. McCall, T. Oka, B. Rachford, P. Sonnentrucker, and D. E. Welty, "Studies of the diffuse interstellar bands. iii. HD 183143," Astrophys. J. **705**, 32 (2009).

[47] J. Zhen, P. Castellanos, D. M. Paardekooper, H. Linnartz, and A. G. G. M. Tielens, "Laboratory formation of fullerenes from PAHs: Top-down interstellar chemistry," Astrophys. J. Lett. **797**, L30 (2014).
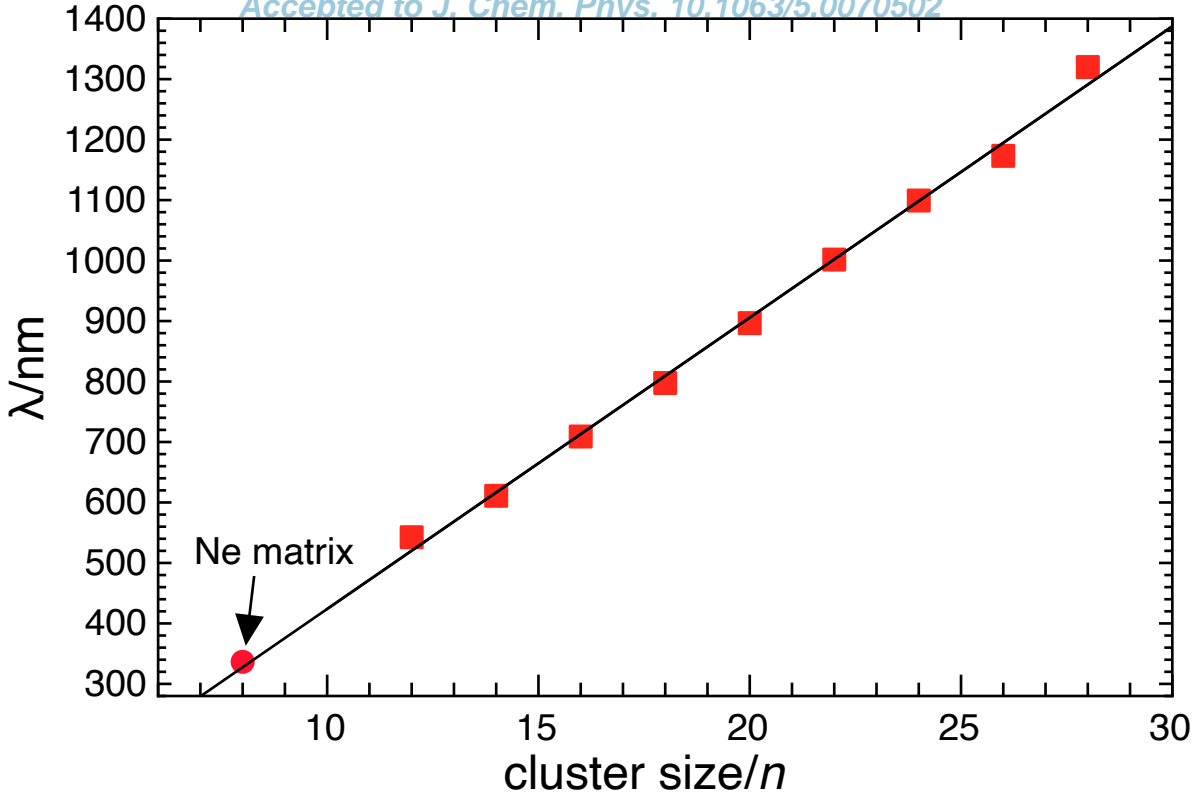
[48]É. Brémond, Á. J. Pérez-Jiménez, C. Adamo, and J. C. Sancho-García, "sp-hybridized carbon allotrope molecular structures: An ongoing challenge for density-functional approximations," J. Chem. Phys. **151**, 211104 (2019).

[49]T. Heaton-Burgess and W. Yang, "Structural manifestation of the delocalization error of density functional approximations: C_{4N+2}^{+} rings and C_{20} bowl, cage, and ring isomers," J. Chem. Phys. **132**, 234113 (2010).

[50]Z. S. Pereira and E. Z. d. Silva, "Spontaneous symmetry breaking in cyclo[18]carbon," J. Phys. Chem. A **124**, 1152–1157 (2020).
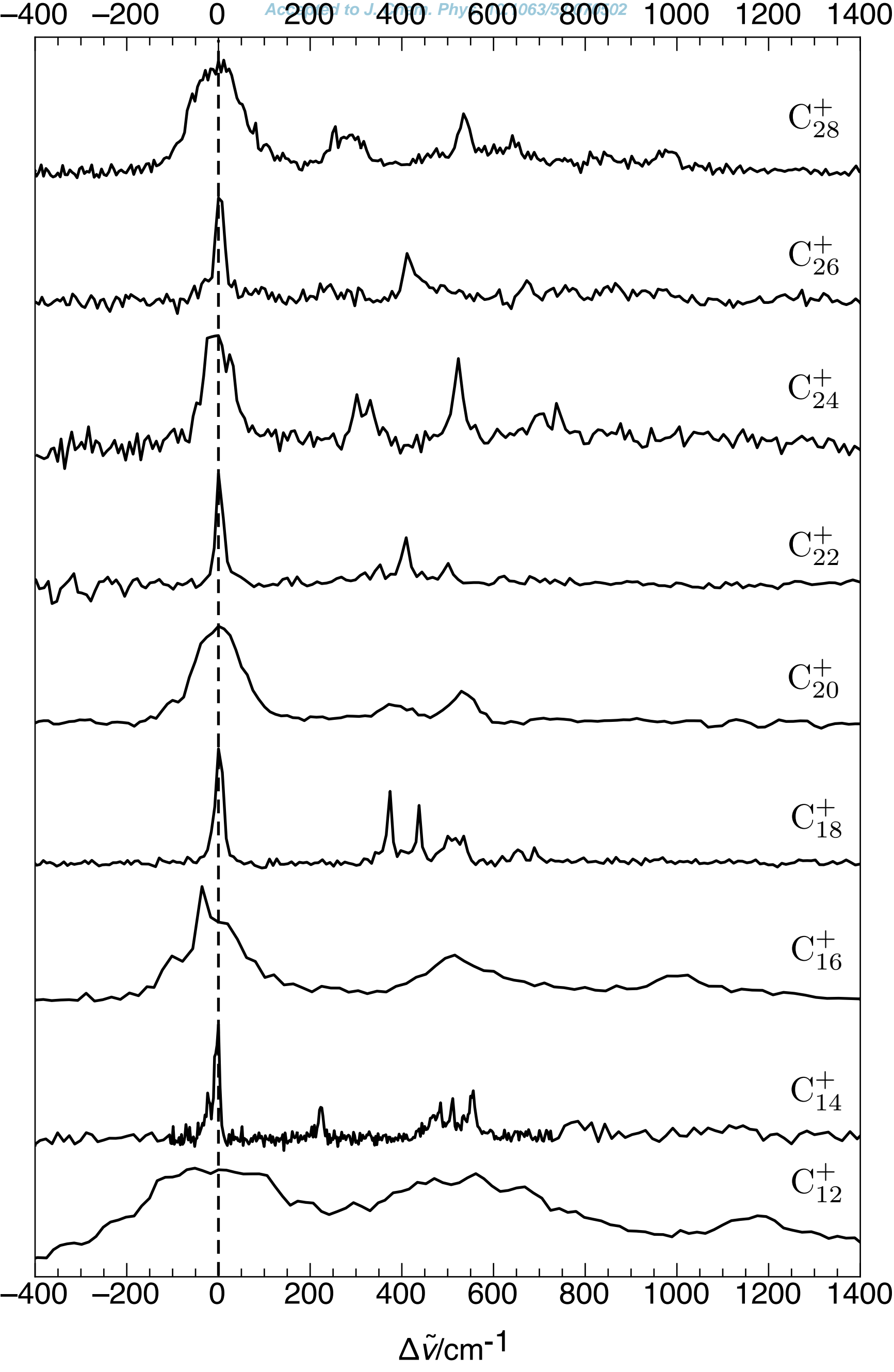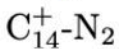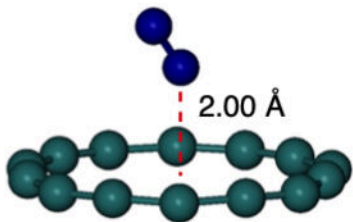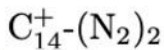
$C_{20}^+-N_2$

C_{20}^+

$C_{20}^+-(N_2)_2$

light-off

photofragment

light-on/off diff
(x4)

photodepletion

26   27   28   29   30

ToF/μs

$\tilde{\nu}/\mathrm{cm}^{-1}$

20000   16000   12000   8000

C_{28}^+

C_{26}^+

C_{24}^+

C_{22}^+

C_{20}^+

C_{18}^+

C_{16}^+

C_{14}^+

C_{12}^+

400   500   600   700   800   900   1000   1100   1200   1300   1400

λ/nm

C_{28}^+

C_{26}^+

C_{24}^+

C_{22}^+

C_{20}^+

C_{18}^+

C_{16}^+

C_{14}^+

C_{12}^+

$\Delta\tilde{v}/cm^{-1}$

C_{14}^+-$(N_2)_2$

2.00 Å

2.01 Å

2.01 Å

C_{14}^+-N_2

$D_0 \approx 791$ cm^{-1}

$D_0 \approx 1566$ cm^{-1}

C_{20}^+-N_2

$D_0 \approx 984$ cm^{-1}